ABLATIVE THERMAL PROTECTION AT LOW HEATING RATES

Ronald B. Pope,* Salvatore R. Riccitiello,
Howard E. Goldstein,** and John A. Parker

Ames Research Center, NASA

Moffett Field, California 94035

Abstract

Evaluation of ablative materials for thermal protection at low heating rates is discussed. Initially, 21 different materials with densities between 255 and 2200 kg/m^3 were evaluated by performing convective heating tests in arc-heated nitrogen streams and observing the backface temperature rise and surface recession. Modified polyurethane foam composite, which has characteristics desirable for ablative thermal protection, was evaluated and excellent insulative performance was demonstrated. Ablative performance of the foam materials is compared with the performance of "state-of-the-art" materials and with analytical predictions.

1. INTRODUCTION

The cone frustum afterbody of the Apollo vehicle is exposed to a mild thermal environment in which convective heating rates are less than 1000 kW/m^2, and the surface pressures are less than about 0.05 atm, during entry into the Earth's atmosphere. Proposed vehicles for which similar thermal environments may exist include probes into the Mars atmosphere and lifting entry bodies. Although these thermal environments are relatively mild, ablative protection appears attractive.

This paper discusses the ablative performance of materials exposed to low-heating-rate environments. The performance of 21 state-of-the-art materials was experimentally evaluated in convective heating environments. These materials have densities between 225 and 2200 kg/m^3 (specific gravity = 0.22 to 2.2), and were evaluated at heating rates to 600 kW/m^2.

A new class of low-density materials is also discussed. Recently, a rigid polyurethane foam composite (designated 5I) with a density of 54 kg/m^3 was developed at Ames to provide both low-temperature thermal protection and fire-suppressant species for aircraft fuel fires.[1] The low density of the materials and their char stability also make them candidates for ablative thermal protection. The ablative performance

*Now a Staff Member-Technical, Sandia Corporation, Albuquerque, New Mexico

**Applied Space Products, Inc., Palo Alto, California

of the materials was therefore evaluated in a convective heating environment at 170 kW/m^2, at a nominal pressure of 0.01 atm.[2] Excellent insulative performance was demonstrated in a nitrogen environment; however, extensive surface removal occurred in an air environment. The foams were modified to provide erosion-resistant surfaces in oxidizing environments. The modified foams were evaluated at heating rates between 170 and 1700 kW/m^2 and at a pressure of 0.01 atm. The performance of the modified foams is discussed and compared with the performance of the state-of-the art materials.

2. EXPERIMENTAL PROCEDURE

Ablative performance of the materials was evaluated by convectively heating blunt ablation samples in arc-heated supersonic flows. The tests were performed in the Planetary Entry Ablation Facility at Ames. Details of the test equipment, procedures, and the date reduction are given in references 3 and 4. Conditions used in this study are shown in Table I.

TABLE I. TEST CONDITIONS

Test condition	Test gas mixture	Total stream enthalpy, mJ/kg	Stagnation-point pressure, atm	Stagnation-point convective heating rate, kW/m^2	Model exposure time, sec	Time heating, kJ/M$_2$
1	N_2	4.4	0.010	170	100	17,000
2	N_2	8.1	.011	340	50	17,000
3	N_2	13.9	.012	570	30	17,000
4	N_2	4.0	.008	170	42	6,940
5	$Ar/N_2/O_2$	1.3	.010	70	60	4,200
6	$Ar/N_2/O_2$	1.3	.010	70	100	7,000
7	N_2/O_2	4.3	.011	170	42	6,940
8	N_2/O_2	6.7	.013	320	22	7,020
9	N_2/O_2	12.0	.013	570	12.5	7,120
10	N_2/O_2	16.0	.015	750	9.5	7,120
11	N_2/O_2	24.0	.018	1020	7	7,140
12	N_2/O_2	55.0	.010	1730	4	6,920

The tests were performed in nitrogen and simulated air environments. To obtain a low heating rate of 70 kW/m^2, the enthalpy of the stream was reduced by heating argon in the arc heater (22 percent by weight of total flow) and adding unheated N_2 and O_2 in the arc-jet reservoir. For heating rates between 170 and 1,020 kW/m^2, only part of the N_2 was heated and the remaining gas was added in the reservoir. For 1,730 kW/m^2, all of the N_2 and O_2 was heated in the reservoir. The ablative specimens were exposed to total heat loads between 4,200 and 17,000 kJ/m^2. As a comparison, the total heat load on the Apollo afterbody is approximately 7,000 kJ/m^2.

The ablative samples were 3-cm-diameter cylinders. The rear face of each specimen was instrumented with a chromel-alumel thermocouple held in place by a 0.05-cm-thick micarta disk bonded to the material with Epoxylite No. 8839 adhesive. Two sample designs were used during the investigation. A schematic of this arrangement is shown in Figure 1.

In the initial model design, Figure 1(a), the ablative sample was bonded to a hollow cylinder of aluminum. The design was used for testing the materials at conditions 1, 2, and 3 (Table I). To minimize heat transfer to the sample support and sting, a modified design, shown in Figure 1(b), was used for all remaining tests. The sample was supported on the sting with three square stainless-steel pins that projected into 0.5-cm-diameter holes drilled in the rear face of the sample. The initial mass per unit area of the samples ($\rho_e X_e$) was varied from 1 to 10 kg/m^2.

The materials were evaluated by inserting the test samples into the centerline of the high-energy supersonic flow and exposing them for the times shown in Table I. The backface temperature was continuously recorded during and after exposure to determine the maximum temperature rise. The temperature of the ablating surface was measured, in some tests, with a monochromatic pyrometer giving an optical or "brightness" temperature at 0.653μ wavelength.

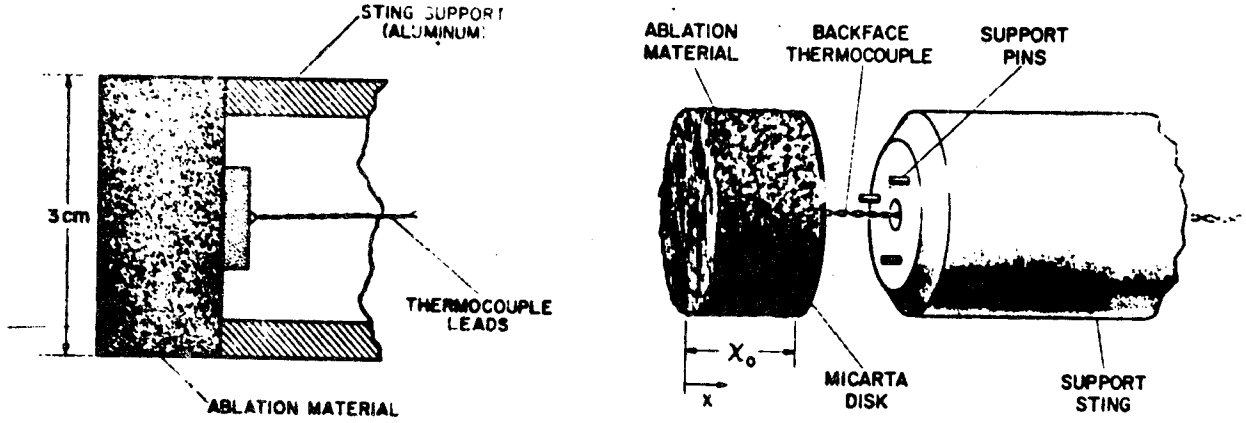

a) ORIGINAL b) MODIFIED

FIGURE 1. SCHEMATIC DRAWING OF TEST SPECIMEN

3. FOAM MATERIAL COMPOSITION

3.1 5I and 5IA FOAM COMPOSITES

The polyurethane binder system used in the formulation was derived from the reaction of alpha methylglucosidepropyleneoxide polyol and a polymeric isocyanate. To this resin system an inorganic salt (potassium fluoborate) and an alkyl halide polymer were added. For the 5I material, the alkyl halide polymer was polyvinyl chloride-acetate copolymer (VMCH). A second polyurethane material (5IA), using the alkyl halide polymer polyvinylidene chloride (Saran A), was also investigated. The compositions are given in Table II.

TABLE II. FOAM COMPOSITION

Material - 5I	Weight percent	Material - 5IA	Weight percent
Polymeric isocyanate	42.11	Polymeric isocyanate	42.11
Methyl glucoside polyol	27.40	Methyl glocoside polyol	27.40
Foaming agent (trichloro mono fluoromethlane - Freon 11)	15.60	Foaming agent (trichloro mono fluoremethlane - Freon 11)	15.60
Surfactant (D.C. 195	0.38	Surfactant (D.C. 195)	0.38
Catalyst (triethylene diamine)	0.59	Catalyst (triethylene diamine)	0.59
Potassium fluoborate	6.96	Potassium fluoborate	6.96
Polyvinyl chloride-acetate copolymer (VMCH)	6.96	Polyvinylidene chloride (Saran A)	6.96

The pyrolysis reaction sequence of 5I foam was defined by thermogravimetric analysis. The degradation proceeds through four identifiable steps, giving a final measured char yield of 26.7 percent.[1] The 5IA system was also developed for fuel fire-protection systems as a complement to the 5I system. Saran A was selected for the alkyl halogenated polymer to provide more fuel fire suppression species in the formulation. In the degradation of Saran A, 2 moles of hydrogen chloride are released per mer unit. The char yield of Saran A at 873° K was 30 percent, which includes 5, 3-percent unremoved halogen from the polymer.

The thermogravimetric analysis of the 5IA system is shown in Figure 2. For the 5IA system, two pyrolysis reactions were observed. The first started at 473° K and ended at 633° K, giving a char yield of 47.8 percent. The calculated char yield for the first process was 47.67 percent, when 1 mole of HCL from the Saran A, 6 moles of H_20, 4 moles of $C0_2$, and all polyol fragments from the urethane polymer system are

eliminated. The second process started at 633° K and ended at 873° K, giving a char yield of 26.9 percent, accounting for initial loss of freon 11. The calculated char yield at 873° K was 25.4 percent, which included the 5.3-percent HCL remaining from the Saran A. As in the 5I system, it was assumed that the inorganic salt and char from the Saran A were retained at 873° K.

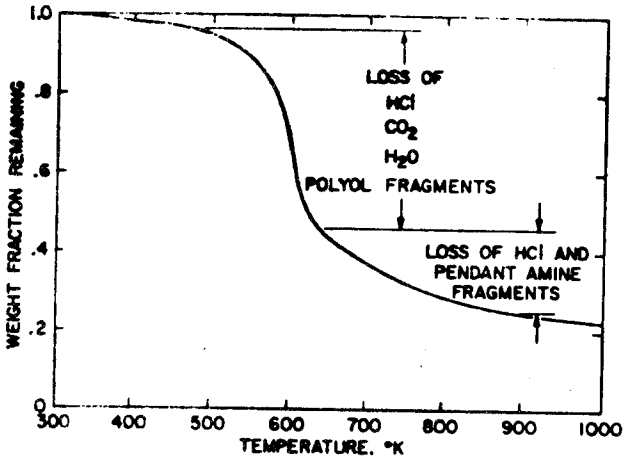

FIGURE 2. THERMOGRAVIMETRIC ANALYSIS OF 5IA FOAM COMPOSITE (3° C/min. in N_2 at 1 atm).

3.2 FOAM MATERIAL MODIFICATIONS

The foam composites were modified with Astroquartz and carbon fibers. The percentage of filler used ranged from 7.5 to 20 percent by weight of the polyurethane foam.

Each material studied is designated in Table III by the initial polyurethane foam used (5I or 5IA), followed by the percentage and designation of the filler material.

The filler material showed no interaction with the basic resin system to increase or decrease the char yield. The variation from theoretical to observed char yield (Table III) was attributed to nonhomogenous distribution of the additives throughout the composite.

The thermograms for the inorganic fiber-filled 5I and 5IA systems are shown in Figures 3 and 4. The only difference observed was a slight shift in the temperature of degradation, which was attributed to the thermal properties of the filler.

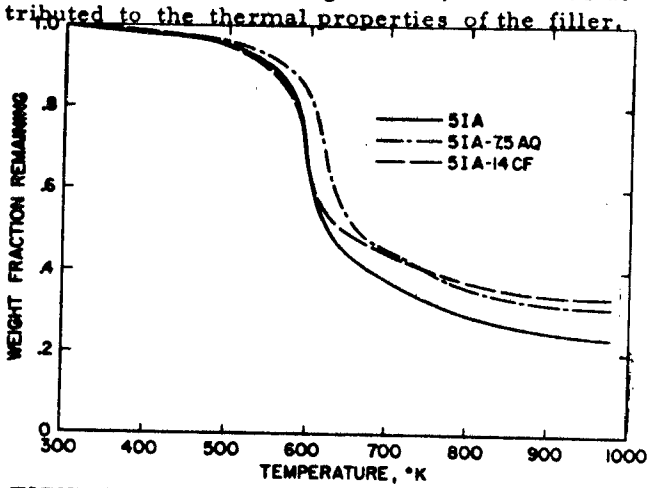

FIGURE 3. THERMOGRAVIMETRIC ANALYSIS OF 5I FOAM COMPOSITES WITH FIBER FILLERS (3° C/min. in N_2 at 1 atm).

Foam composites with impregnated fabric surfaces were fabricated. The unfilled 5I foam and the carbon-fiber-filled 5IA-14CF foam composites were also placed in a high-temperature phenolic-fiberglas honeycomb structure (Hexcel HRP 3/8 GF-11 2.2). The measured properties of the foam composites are compared with the properties of Avco 5026-39HCG and Martin SLA-561 in Table IV.

TABLE III. FOAM MODIFICATIONS

Foam type	Composition	TGA char yield at 873° K under N_2	
		Theoretical	Measured
5I	See Table II	26.4	26.7
5IA	See Table II	25.4	26.9
5IA-20CF	5I+20 percent carbon fiber	41.4	41.9
5IA-14CF	5IA+14 percent carbon fiber	35.8	36.3
5I-10AQ	5I+10 percent Astroquartz fiber	34.1	34.0
5IA-7.5AQ	5IA+7.5 percent Astroquartz fiber	31.0	33.1

The thermal conductivity of the 5I foam was measured on a guarded hot plate and found to be approximately 1.4 to 3.3 W-cm/m^2 ^oK for temperatures between 298^o and 398^o K. The thermal conductivity of SLA-561 is 5.2 W-cm/m^2 ^oK[5] and of 5026-39HCG is 11.5 W-cm/m^2 ^oK. (6)

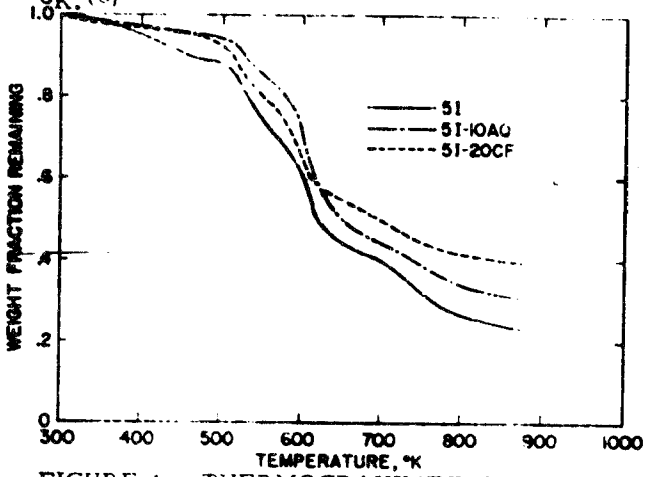

FIGURE 4. THERMOGRAVIMETRIC ANALYSIS OF 5IA FOAM COMPOSITE WITH FIBER FILLERS (3° C/min. in N_2 at 1 atm).

The 21 heat-shield materials initially evaluated are listed in Table V. The materials were considered to represent the state-of-the-art for low-heat-rate environments. All materials were evaluated with one initial thickness at conditions 1, 2, and 3 (Table I). In addition, six materials were evaluated with varying thicknesses. Avco 5026-39HCG and the Martin SLA-561 were evaluated at conditions other than 1, 2, and 3.

A large quantity of data was obtained during this evaluation. Therefore, a correlation of the data where the performance of the materials can be compared and evaluated would demonstrate which materials were superior and how material properties could be altered effectively to improve material performance. Accordingly, the semi-empirical correlating method of Mezines[8] was considered. Mezines' analysis used the following assumptions:

(1) one-dimensional heat flow
(2) small geometric changes in the material as a result of ablation
(3) constant thermal properties
(4) small effect of enthalpy and pressure of material performance

TABLE IV. MATERIAL PROPERTIES

Material	Bulk density, kg/m^3	Open cell porosity, percent	Compressive strength (a), Newton X 10^{-4}/m^2	Initiation temperature of decompression, ^oK
Avco 5026-39HCG	512	54.6	1576.60	593
Martin SLA-561	225	43.5	47.56	523
Ames 5I	54	3.3	21.03	498
5IA	104	6.1	36.54	473
5IA-20CF	102	12.6	25.60	483
5IA-14CF	104	5.90	33.09	473
5I-10AQ	100	14.7	19.06	498
5IA-7.5AQ	180	12.5	50.33	498

4. MATERIAL EVALUATION

4.1 STATE-OF-THE-ART MATERIAL EVALUATION

The properties of ablative materials which are important for thermal protection and were considered during the investigation include: (1) low thermal conductivity to minimize heat transfer to the vehicle substructure; (2) low density to minimize the heat-shield weight; (3) a charred surface to resist erosion in oxidizing environments and to radiate a large portion of the input energy; and (4) production of gaseous species to block convective heat transfer.

(5) surface temperature - initial temperature
(6) constant heat input at the surface

The correlation thus obtained gave the initial weight per unit area, ρX_e, required to limit the backface temperature to a specified value for a given material, heating rate, and total heat load. The effectiveness of different materials was then determined experimentally using the correlation.[8]

However, the data of the present study were obtained by testing models of different materials

and thicknesses at specific heating rates and he heat loads. The maximum temperature rise was observed. For many of the tests, the transit time of the heat pulse through the material was nearly equal to or exceeded the exposure time; that is, the major portion of the temperature increase at the backface occurred after the heat pulse.

TABLE V. MATERIALS FOR INITIAL EVALUATION

		Density, kg/m^3	Test conditions
1.	Avco 5026-39HCG*	512	1, 2, 3, 4, 6, 7
2.	Avco 5026-99*	390	1, 2, 3
3.	Avco 5026-39-P8	535	1, 2, 3
4.	Avco Mod 5*	683	1, 2, 3
5.	Avco Mod 7	683	1, 2, 3
6.	Avco Mod 20	683	1, 2, 3
7.	Martin SLA-561*	225	1, 2, 3, 4, 6, 7, 8
8.	Low-density phenolic nylon[7]	580	1, 2, 3
9.	McDonnell D-45-RF	598	1, 2, 3
10.	McDonnell D-45-RHF	648	1, 2, 3
11.	McDonnell BR-46	587	1, 2, 3
12.	McDonnell BR-47	405	1, 2, 3
13.	Lockheed quartz fiber	249	1, 2, 3
14.	General Electric 1004AP	631	1, 2, 3
15.	General Electric 1004AP*	357	1, 2, 3
16.	Armstrong Cork 2755*	502	1, 2, 3
17.	Avco cork silicone 893-23	455	1, 2, 3
18.	Teflon	2200	1, 2, 3
19.	Avco foamed teflon	752	1, 2, 3
20.	Avco foamed teflon	542	1, 2, 3
21.	Boeing polyborazole	562	1, 2, 3

*Multiple model thicknesses were tested.

The correlation was therefore modified by assuming that the maximum backface temperature was proportional to some power of the temperature increase at the termination of the heat pulse. The following relationship results:

$$\Delta T_{max} \sim \propto \left[\frac{\theta q^{1/4}}{\chi_o^2}\right]^{\beta} \qquad (1)$$

where ΔT_{max} = maximum backface temperature rise, $\propto$ and β are constants to be determined experimentally for each material, θ is the heating duration, q is the heating rate, and χ_o is the initial material thickness. Note that equation (1) gives ΔT_{max} independent of the material density ρ_o. The weight per unit is given by

$$W/A = \rho_o \chi_o$$

and equation (1) can be written:

$$T_{max} = \propto \left[\frac{\theta q^{1/4} \rho_o^2}{(W/A)^2}\right]^{\beta} \qquad (2)$$

The parameter $(\theta q^{1/4}/\chi_o^2)$ successfully correlated the data for materials 1 through 15, Figure 5, at conditions where the surface recession was less than 10 percent of χ_o (see assumption 2). Other data for Martin SLA-561[9] are also included in Figure 5. Thus, Figure 5 represents data for 13 materials, 3 test sample designs, 3 gas mixtures, and a wide range in χ_o, q, and θ. This broad spectrum of data was correlated with ±30 percent by the relationship:

$$\Delta T_{max} = 0.169 \left[\frac{\theta q^{1/4}}{\chi_o^2}\right]^{0.43}$$

The data for the GE 1004 AP material was correlated by the relationship of equation (1). Although large values of surface recession were observed for materials 16 through 21, the data fit the relationship of equation (1) except for the Boeing Polyborazole. Values for $\propto$ and β in equation (1) are summarized in Table VI for materials 1 through 20.

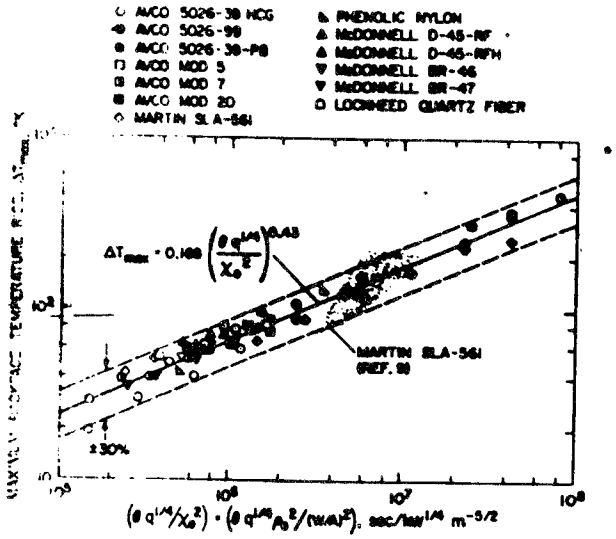

FIGURE 5. DATA CORRELATION FOR MATERIALS 1-13.

conditions, giving low backface temperatures and also being highly resistant to surface removal.

(b) Both 5I-20CF and 5IA-14CF performed satisfactorily at 170 kW/m^2, but the surface removal increased rapidly above 170 kW/m^2.

(c) The materials with impregnated fabric surfaces did not perform satisfactorily. The material underneath the fabric surfaces was consumed, causing delamination and elimination of the fabric from the models.

(d) The materials in honeycomb exhibited rough surfaces, excessive surface recession in each individual honeycomb cell, and high backface temperatures.

The data for the 5I, 5I-10AQ, 5I-20CF, and 5IA-7.5AQ materials, for conditions where surface recession was small, were correlated

TABLE VI. CORRELATION CONSTANTS FOR MATERIALS 1 THROUGH 20

Material	α	β
1-13	0.169	0.43
14-15	.097	.51
16-17	1.67	.23
18-20	.022	.55

4.2 FOAM MATERIAL EVALUATION

4.2.1 Experimental

All the foam materials were initially exposed to condition 7 (170 kW/m^2). The performance of each was evaluated, and those materials that performed satisfactorily at this condition were then exposed to the next higher heating rate. Evaluation and elimination were repeated at each condition. In addition, some materials were tested at conditions 4, 5, and 6.

The performance of each material was evaluated on the basis of (1) maximum backface temperature; (2) surface recession; and (3) visual appearance of char following exposure. A summary of the performance of the materials follows:

(a) Both 5I-10AQ and 5IA-7.5AQ performed very well at all heating

using equation (1). The results are shown in Figure 6. For α = 0.169 and β = 0.43, the data were correlated to within ± 30 percent, thereby allowing a direct comparison between the foam materials and materials 1-13. As previously discussed, heat-shield weight is directly proportional to the density of the materials for a constant heating-rate environment and backface temperature. Hence, a substantial decrease in the required heat-shield weight can be realized by using a modified polyurethane foam. For the data presented, the weight of a 5I-10AQ heat shield would be 85 percent less than for a heat shield of Avco Mod 5, 81 percent less than for Avco 5026-39HCG, and 54 percent less than Martin SLA-561 as illustrated in Figures 5 and 6.

4.2.2 Theoretical

The correlation represented by equation (1) has permitted a comparison of the performance of

different materials when exposed to a constant heating rate. However, an analysis that predicts ablative performance of different materials when exposed to time-varying heating rates would be required for detailed design of a heat shield. The analysis should provide details such as the time variation of temperature within the ablator. One such analysis is the CMA computer program[10] that was used to predict the measured performance of the foam materials. The CMA program uses material properties and a numerical solution of the transient one-dimensional thermal response equations for an ablative material to obtain temperature and material consumption histories. If the analytical model satisfactorily predicts the measured performance, the model should also be valid for time-varying conditions having similar heating rates, total heat loads, and surface pressures.

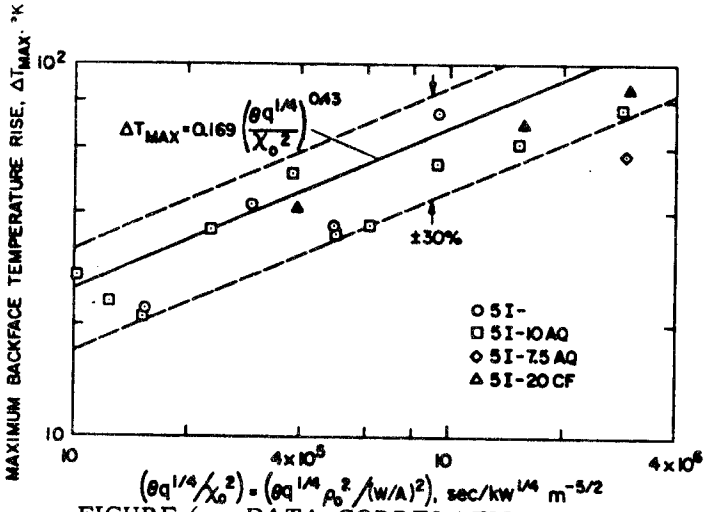

FIGURE 6. DATA CORRELATION FOR FOAM MATERIALS.

The following thermophysical and thermochemical properties of the virgin material and char are required: density, pyrolysis gas enthalpy, pyrolysis gas composition, heat of pyrolysis, heats of formation of the components, pyrolysis kinetic parameters, specific heat, thermal conductivity, char emittance, and surface erosion kinetics.

The virgin material density and char yield of the foam composites are given in Tables III and IV.

The thermochemical terms (gas enthalpy, heat of pyrolysis, and heats of formation) are only significant in that they must be reasonable approximations (± 25 percent) to the true values and must be consistent with the boundary-layer chemistry. As a first approximation, the heat of pyrolysis for phenolic nylon and the corresponding gas enthalpies and heats of formation were used.

A simple one-step rate equation determined from the TGA data was used for the pyrolysis kinetics.

Specific heat of polyurethane and silica were used for the virgin material. The proper weighted sum of carbon and silica specific heats was used for the char.

The surface emittance of ablating 5I-10AQ specimens was measured at a temperature of about 2200° K using the equipment and method discussed in reference (11) and was found to be approximately 0.5. This value was used in the calculations.

Thermal conductivity of the foam is the most significant thermophysical property in a mild heating environment. Initially, the thermal conductivity of the virgin material as measured with a guarded hot plate was used in the calculations. Char conductivity was assumed to increase as the cube of the temperature. The internal temperature response of a 1-inch-thick 5I foam sample exposed to a fuel fire was predicted with the charring material ablation program using the above properties. Using conductivities obtained by the guarded hot plate technique, extremely low internal temperatures were predicted. Conductivity was then varied until good agreement was obtained between the measured and calculated temperatures. The derived virgin conductivity was approximately 10 W-cm/m^2 °K; char conductivity at 1600° K was approximately 37.4 W-cm/m^2 °K. The apparent disparity between measured conductivity and estimated conductivity was that the effective conductivity used in the ablation model includes the effect of radiant heat transfer within the material. In a low-density, low-conductivity material, a significant fraction of the heat transfer may occur by radiation because conduction through the solid is small and the material is often transparent to infrared radiation. Calculations showed that the conductivity chosen could be used for all the foams tested. This resulted from radiation being the predominant means of heat transfer in the foams. If solid conduction predominated, doubling the density should double the conductivity. This did not occur.

The surface recession of the foam composites was computed. For those foams not reinforced with silica, reasonable estimates of the erosion

could be computed for most test data. The computations were made assuming that surface recession occurred by diffusion controlled oxidation and that the conditions were quasisteady state.[12] Results for the available data are presented in Table VII. Correlation between data and theory was reasonable. The nominal properties used in the analysis are given in Table VIII. For internal temperature response between materials.

TABLE VII. SURFACE RECESSIONS OF FOAMS

Material	Heating condition	Heat flux kW/m^2	Surface recession, cm	
			Measured	Calculated
5I	7	170	1.8-1.9	1.52
5IA	7	170	.75	.76
5I-20CF	8	320	.38	.36
5IA-14CF	7	170	.20	.63
	8	320	.20	.42
	9	570	.33	.23

TABLE VIII. NOMINAL THERMOPHYSICAL PROPERTIES OF FOAM MATERIALS

Property	Virgin material	Char
Thermal conductivity, W-cm/m^2 $^\circ$K	10.0	37.4*
Specific heat, J/kg $^\circ$K	1425	1630*
Density, kg/m^3		
5I-10AQ	100	34
5I-7.5AQ	180	60
5IA-14CF	104	37
Heat of pyrolysis, MJ/kg	.116	---
Heat of formation, MJ/kg	-2.56	0.116
Emittance	---	.5

*At 1660° K

Typical measured and predicted backface temperature histories for 5I-10AQ models are shown in Figures 7 and 8 for test conditions 7 and 8 for test conditions 7 and 9, respectively.

The temperature variation is adequately predicted to within $\pm$20 percent.

Figure 9 shows the predicted and measured variation of maximum backface temperature with applied heating rate. The data are for a total heat load of approximately 7000 kJ/m^2 (conditions 7-12) and for values of $\rho_o \chi_o$ of 1 and 2kg/m^2. The calculations and experimental data for $\rho_o \chi_o$ = 2 kg/m^2 agreed well over the entire heat-flux range. At low heat fluxes, there is some divergence between the calculations and the data for $\rho_o \chi_o$ = 1 kg/m^2. This discrepancy is not presently accounted for in that the calculations give a higher temperature than the measured values.

The variation of surface temperature with applied heating rate is shown in Figure 10. Two curves are compared with the data. First, the solid line represents the energy radiated from the surface when the char is assumed to be a graybody radiation with ϵ = 0.5 (Table VIII). The dashed curve is the temperature calculated from the CMA computer analysis. The agreement between the measurements and calculations was excellent.

The preceding indicates that the analytical method can be used to adequately predict the response of the foam materials when surface recession is small. However, until similar comparisons are performed at higher heating rates and total heat loads, the analysis cannot be considered valid for more severe conditions.

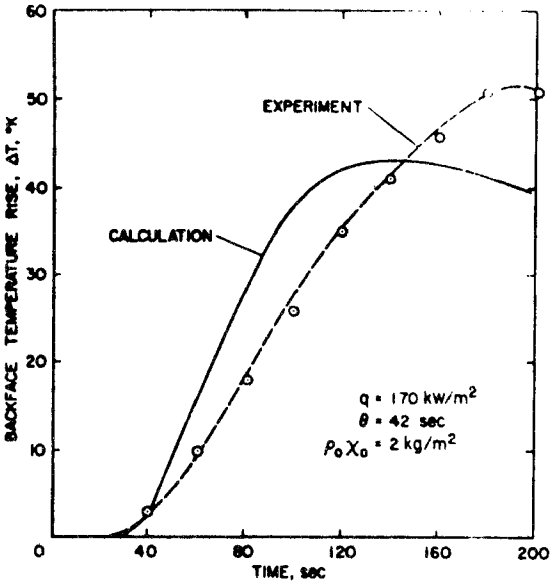

FIGURE 7. BACKFACE TEMPERATURE HISTORY FOR 5I-1AQ, CONDITION 7.

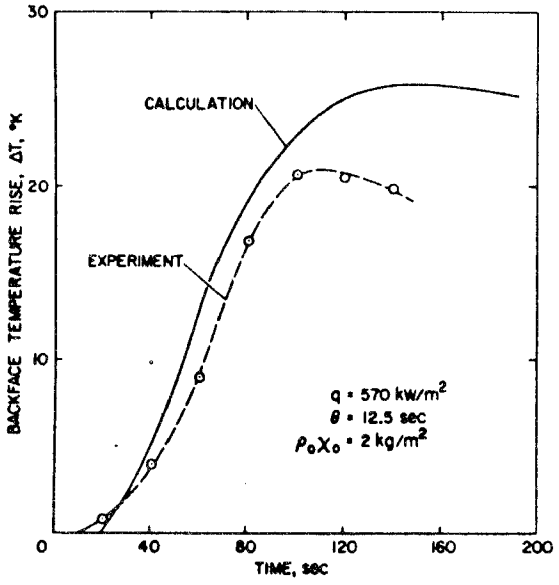

FIGURE 8. BACKFACE TEMPERATURE HISTORY FOR 5I-10AQ, CONDITION 9.

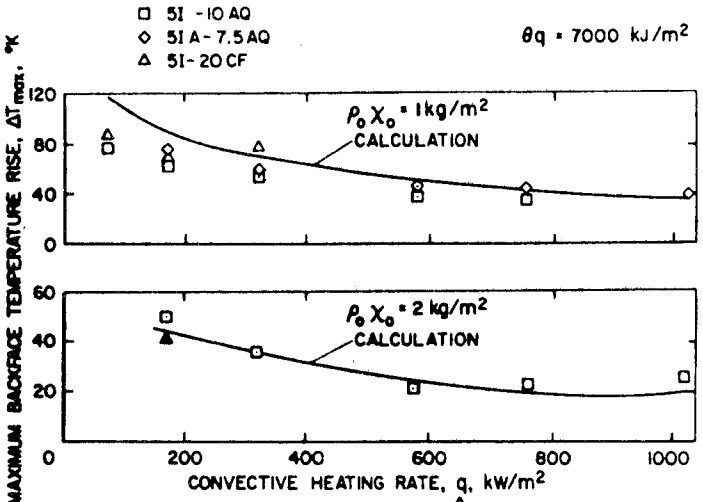

FIGURE 9. VARIATION OF ΔT_{max} WITH HEATING RATE, CONSTANT TOTAL HEAT LOAD.

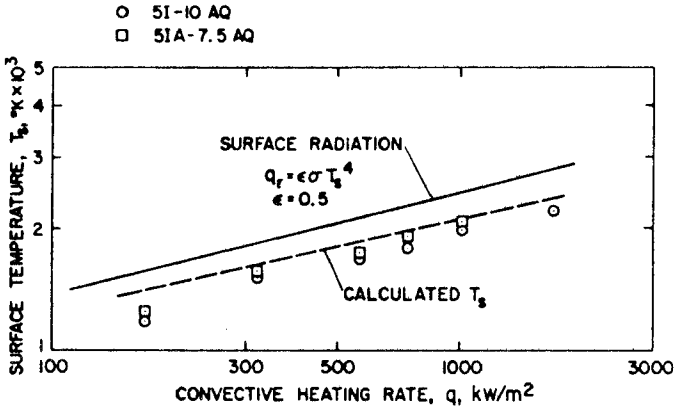

FIGURE 10. VARIATION OF SURFACE TEMPERATURE WITH HEATING RATE.

4.3 DISCUSSION OF FOAM COMPOSITES

The Astroquartz fibers, when placed in the polyurethane foam, provided high-temperature surfaces that resisted removal during the ablation process in oxidizing environments. This resistance was far superior to that exhibited by the other modified polyurethane foam composites. Qualitatively, the chars of 5I-20CF were rigid at low temperature and became weak at the higher temperatures (1700°-1900° K). In contrast, the 5I-10AQ char was initially rigid, became weak at a temperature of about 1500° K, but again became rigid at temperatures above 1700°K. Similarly, the 5IA-7.5AQ char became weak at a temperature of about 1700° K, but again became rigid at temperatures above 1950° K.

char produced by 5I-10AQ at different temperature levels are shown in Figure 11. At 1170° K, the surface appears to be a mixture of the charred SI material and Astroquartz fiber. At 1540° K, the surface is composed mainly of Astroquartz fibers. At 2000° K, the Astroquartz fibers have apparently interacted with the charred material, forming a rigid surface. The char of 5I-10AQ was always stronger and more homogenous than the char of 5IA-7.5AQ. The Astroquartz began to melt at approximately 2200° K. The erosion resistance could possibly result from a reaction at high temperature of the Astroquartz with boron from the potassium fluoborate and carbon residue from the polymer to form a pseudo borosilicon carbide structure.

FIGURE 11. POSTRUN PHOTOGRAPH OF 5I-10AQ SPECIMENS.

Support for the interaction of the boron and the other ingredients in the char is demonstrated in Figure 12. This figure shows the quantitative analysis percentage of boron, fluorine, silicon, and carbon remaining in the char after exposure to the selected thermal environments. As indicated, the boron is introduced into the composites as potassium fluoborate. The data show that the percentage of boron in the char layer remains relatively constant over the selected thermal environments. The maximum theoretical percent of boron that could remain in the char of 5I-10AQ is 2.1 percent if a char yield of 30 percent is assumed. This shows that little boron was volatized from the composite.

The percentage of fluorine does not remain over the thermal environment investigated, but actually decreases. The decrease in the percentage of fluorine in the char indicates that the boron fluoride was cracked to give free fluorine and boron.

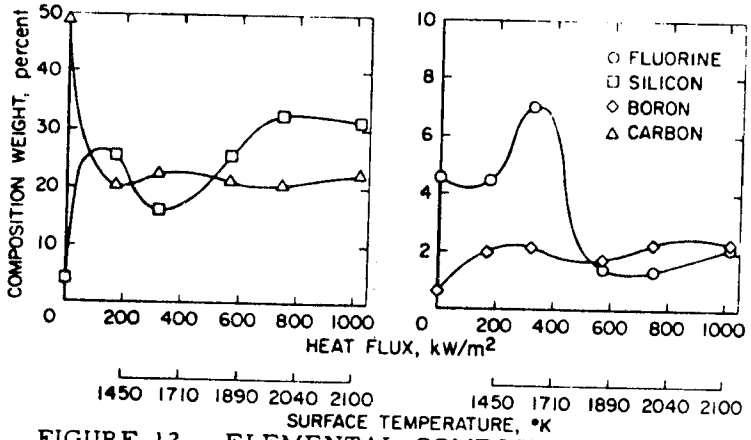

FIGURE 12. ELEMENTAL COMPOSITION OF 5I-10AQ SPECIMENS.

As can be seen from Figure 12, the percentage of carbon remains relatively constant over the range investigated. For silicon, the percentage increased as the heat flux increased. The amount of silicon at the higher heat-flux conditions indicates that most of the silicon remained in the char. The theoretical maximum percentage of silicon in char was calculated to be 16.5 percent if a char yield of 30 percent is assumed. The increase in the amount of silicon with heat flux and the fact that most of the boron remained in the char indicate a possible interaction between the boron and silicon.

5. CONCLUSIONS

The weight of a heat shield for a low-heating-rate environment can be significantly reduced by using low-density materials. For the materials investigated, the reduction in weight is approximately proportional to the reduction in material density. The weight of a heat shield could be reduced by at least 50 percent in the described environments if a modified polyurethane foam composite (5I-10AQ) were used rather than the state-of-the-art materials discussed.

Surface erosion of the polyurethane composites can be minimized by the addition of inorganic Astroquartz fibers to the foam. This addition does not increase the material density of the composite excessively. Thus, it appears that the polyurethane foams with Astroquartz fibers are potential heat-shield materials for heating rates to approximately 1700 kW/m^2 and total heat loads of 7000 kJ/m^2. ■

References

1. J. A. Parker et al., "Development of Polyurethane as Thermal Protection Systems for Control of Fuel Fires in Aircraft Structures." Presented at the 25th Annual Conference of Society of Plastic Industries, May 1-3, 1968, San Francisco, Calif.

2. R. B. Pope et al., "Evaluation of a Polyurethane Foam for Ablative Protection at Low Heating Rates." Journal of Spacecraft and Rockets, accepted for publication.

3. R. B. Pope, "Measurements of Enthalpy in Low Density Arc-Heated Flows." AIAA Journal, 6, 103-110 (1968).

4. R. B. Pope, "Stagnation Point Convective Heat Transfer in Frozen Boundary Layers" AIAA Journal, 6, 619-626 (1968).

5. E. L. Strauss, "New Ablative Heat Shield Materials for Mars Landers." 1967 SAE Transactions, Society of Automotive Engineers, Inc., New York.

6. G. Strouhal, et al., "Thermal Protection System Performance of the Apollo Command Module." AIAA/ASME Seventh Structures and Materials Conference, Cocoa Beach, Florida, April 18-20, 1968.

7. J. A. Parker, "Needs of Characterization and Process Control of Low-Density Composites for Aerospace Application." Plastics in Government, Picatinny Arsenal, Doven, N. J., July 1966, pp. 31-46.

8. S. A. Mezines, "A Seim-Empirical Method for Correlating the Thermal Performance of Charring Ablative Materials." AIAA Paper 68-767.

9. E. L. Strauss, "Response of Superlight Ablators to Various Heat Pulses." AIAA Paper 68-301.

10. R. A. Rindal et al., "Analytical and Experimental Study of Ablation Material for Rocket Engine Application." NASA CR-54757, 1966.

11. R. B. Pope, "Measurements of the Total Surface Emittance of Charring Ablators," AIAA Journal, 5, 2285-2286 (1967).

12. K. M. Kratsch et al., "Theory for the Thermophysical Performance of Charring Organic Heat Shield Composites." Rept. LMSC-803099, Oct. 18, 1963.

MANUFACTURE AND PROPERTIES OF SMALL DIAMETER TUNGSTEN ALLOY TUBING

A. Milner and D. W. Voegeli

3 M Company

Abstract

Recent advances in Aerospace and Nuclear Technology have created a demand for precision tungsten tubing for ultra-high temperature service. Three processes by which tungsten tubing can be fabricated are outlined and the product property characteristics of each method reviewed. Particular attention is given to a newly developed technique for the direct conversion of metal powder to finished tubing which exhibits unusual high temperature structural stability.